



UPPSALA  
UNIVERSITET

DiVA 

<http://uu.diva-portal.org>

This is an author produced version of a paper published in *Journal of Electroanalytical Chemistry*. This paper has been peer-reviewed but does not include the final publisher proof-corrections or journal pagination.

Citation for the published paper:

Waita, S.M et. al.

"Electron Transport and Recombination in Dye Sensitized Solar Cells Fabricated from Obliquely Sputter Deposited and Thermally Annealed TiO<sub>2</sub> Films"

*Journal of Electroanalytical Chemistry*, 2007, Vol. 605, Issue 2: 151-156

[URL: http://dx.doi.org/10.1016/j.jelechem.2007.04.001](http://dx.doi.org/10.1016/j.jelechem.2007.04.001)

Access to the published version may require subscription.

Published with permission from: Elsevier



## **Electron transport and recombination in dye sensitized solar cells fabricated from obliquely sputtered and thermally annealed TiO<sub>2</sub> films**

S. M. Waita<sup>a</sup>, B. O. Aduda<sup>a</sup>, J. Mwabora<sup>a</sup>, C. G. Granqvist<sup>b</sup>, S.-E. Lindquist<sup>b</sup>, G. Niklasson<sup>b</sup>, A. Hagfeldt<sup>c</sup> and G. Boschloo<sup>c\*</sup>

<sup>a</sup> Department of Physics, University of Nairobi, P.O Box 30197, Nairobi, Kenya.

<sup>b</sup> Department of Engineering Sciences, Solid State Physics, The Angstrom Laboratory, Uppsala University, P.O. Box 534, SE-75121 Uppsala, Sweden.

<sup>c</sup> Center of Molecular Devices, Department of Chemistry, Royal Institute of Technology, Teknikringen 30, SE-100 44 Stockholm, Sweden.

### **Abstract**

The properties of dye-sensitized solar cells based on annealed titanium dioxide films prepared by oblique reactive DC magnetron sputtering have been studied in detail. Electron transport and recombination were studied using intensity-modulated photocurrent and photovoltage spectroscopy (IMPS and IMVS), respectively. Both the electron transport and lifetime were found to decrease with light intensity but increased with the thickness of the TiO<sub>2</sub> thin film. The properties are very similar to those observed for solar cells based on colloidal TiO<sub>2</sub> films, although their morphologies are very different. In all cases films are composed of a porous assembly of TiO<sub>2</sub> nanocrystals. Grain boundaries with associated trap and / or energy barriers are the likely cause of the observed transport properties.

\* Corresponding author. Tel. +46 8 790 8178. E-mail: [gerrit@kth.se](mailto:gerrit@kth.se) (G. Boschloo)

## **Introduction**

Dye sensitized solar cells (DSSC) based on nanocrystalline  $\text{TiO}_2$  have been named as a possible low-cost alternative to conventional silicon-based photovoltaics [1, 2].

Grätzel and co workers have achieved solar power to electrical conversion efficiencies for DSSCs exceeding 10 % [2]. The structure and working mechanism of DSSC differs completely from conventional photovoltaics. It makes use of a thin film of a porous nanocrystalline  $\text{TiO}_2$  onto which a dye is adsorbed whose purpose is to harvest solar radiation. On irradiation, photoexcited electrons are injected from the dye into to the  $\text{TiO}_2$  conduction band and transported to the back contact and the external circuit. Iodide ions in the electrolyte reduce the oxidized dye. Finally, the triiodide ions formed in this reaction are reduced to iodide at the platinized counter electrode.

Charge collection in the DSSC is surprisingly efficient, considering that injected electrons travel relatively slowly towards the substrate by diffusion, always in close proximity to electron acceptors present in the electrolyte. Transport studies have shown that electrons transport is strongly light intensity dependent [3-6]. Electron transport properties are therefore best studied using techniques such as intensity modulated photocurrent spectroscopy (IMPS), where a small sinusoidal light intensity is superimposed on a larger steady background level illuminating the solar cell [3-6]. A closely related technique, intensity-modulated photovoltage spectroscopy (IMVS) is used to measure electron lifetime under open circuit conditions [7].

Several studies have focused on the effect of the nanocrystalline  $\text{TiO}_2$  film on the electron transport. For instance, the porosity was found to play an important role, as it

affects the number of connections between neighboring particles and the number of dead-ends [8]. Electron transport was therefore found to be slower in more porous films. Also the TiO<sub>2</sub> particle size has been investigated: increasing size was found to lead to faster electron transport and slower recombination [9].

While most work has been done on films prepared using TiO<sub>2</sub> colloids, other methods are also suitable to obtain films for DSSCs. Oblique deposition of TiO<sub>2</sub> by sputtering [10, 11] or electron beam evaporation [12] yields porous TiO<sub>2</sub> films. Highly porous tree-like structures have been made by reactive sputter deposition on rotating substrates [10, 11]. We will show here that porous columnar TiO<sub>2</sub> films are formed by oblique sputtering without rotation, which are suitable as electrodes in DSSCs after thermal annealing. Furthermore, we will report on the electron transport and recombination in such films.

## **Experimental Section**

**Film preparation and characterization:** Film preparation for the working electrode was done in two stages: sputtering and subsequent thermal annealing. Reactive DC magnetron sputtering was carried out in a Balzers UTT 400 vacuum chamber equipped with a turbo molecular pumping system. A titanium metal disc (5 cm in diameter and 0.625 cm thickness) and purity 99.9 %, was used as both target and cathode, while the substrate was maintained as the anode. A constant DC current of 750 mA at power of ~ 385 W, was applied to the target. After pumping down to ~10<sup>-7</sup> mbar, Argon gas (99.998%) was introduced into the sputtering chamber at 100 ml/min. To remove surface contaminants on the target, pre-sputtering was done for ~10 minutes in pure argon gas. Oxygen ((99.998%), the reactive gas was then

introduced into the chamber. The argon-oxygen gas ratio was maintained at 0.02 while the working pressure was ~12 mTorr. The average TiO<sub>2</sub> deposition rate was ~18 nm min<sup>-1</sup>. Transparent fluorine-doped tin oxide (FTO) coated glass substrates (Hartford Glass Company, Inc.) with a sheet resistance of 8 Ω/square were used. A vacuum tape was used to keep the substrates fixed onto the substrate holder and provide a step for film thickness determination. The substrates were positioned ~ 11.5 cm from the target at a 60° angle between the direction of the sputter beam and the substrate normal. The substrate was neither heated nor rotated during the deposition process.

The films were annealed in air ~ 450 °C for ~4 hrs using a programmable furnace (Nabertherm) to obtain the desired stoichiometry and crystallinity of titanium dioxide. The annealing temperature was above the amorphous - crystalline anatase titanium oxide transition temperature (~350 °C) but below the standard glass transition temperature of ~550 °C. The samples were removed from the oven after cooling to room temperature. The film thickness was determined using a Tencor Alpha-step 200 surface profilometer. A Siemens D5000 diffractometer with Cu anode and grazing incidence unit was used for X-ray diffraction (XRD).

### **Solar cell fabrication**

The prepared TiO<sub>2</sub> films were heated at ~450 °C for ~10 minutes to remove possible contaminants such as water vapor and allowed to cool down to ~ 80 °C before immersion into the dye complex (0.5 mM bis(tetrabutylammonium)cis-bis(thiocyanato)bis(2,2'-bipyridine-4-carboxylicacid,4'-carboxylate) ruthenium(II)), commonly referred to as N719 (Solaronix S.A) in ethanol solution for a day. Excess

dye was removed by rinsing with ethanol. The counter electrode was thermally platized FTO glass, prepared by spreading  $\sim 10 \mu\text{l}$  of 5 mM  $\text{H}_2\text{PtCl}_6$  in isopropanol on a conducting glass substrate and heating in air at  $\sim 380^\circ\text{C}$  for  $\sim 10$  min. The working and counter electrode were sandwiched using a frame of thermoplastic (Surlyn 1702) and were laminated for  $\sim 1$  min at  $\sim 100^\circ\text{C}$  in vacuum. The electrolyte (0.5M LiI, 0.05 M  $\text{I}_2$  and 0.5 M 4-tert-butyl pyridine in 3-methoxypropionitrile (3-MPN) was introduced through a hole in the counter electrode that was sealed afterward. Electrical contacts were made by applying silver paint (Leitsilber, Hans Wolbring GbmH). The active area of the cell was  $0.785 \text{ cm}^2$ . Three solar cells were fabricated herein designated as cell 1, fabricated from a  $3 \mu\text{m}$   $\text{TiO}_2$  film, cell 2, fabricated from a  $6.7 \mu\text{m}$   $\text{TiO}_2$  film and cell 3, fabricated from a  $10 \mu\text{m}$   $\text{TiO}_2$  film.

IMPS and IMVS measurements were carried out using illumination from a diode laser ( $\lambda=635 \text{ nm}$ ). The solar cell was connected directly to a lock-in amplifier (Stanford Research Systems SR 830) in case of IMVS, or via a low noise current amplifier (Stanford Research Systems SR 570) in case of IMPS. The intensity of the incident laser light was measured using a calibrated silicon diode. All measurements were performed in a closed black metallic box. The solar cells were illuminated from the titanium oxide substrate side (SE illumination).

## **Results and discussion**

Figure 1 shows X-ray diffraction (XRD) patterns for the sputtered titanium dioxide films. As-deposited films are amorphous; the observed peaks are related to the FTO back contact coating. Films annealed at  $450^\circ\text{C}$  are crystalline and consist only of the anatase phase of  $\text{TiO}_2$ . These findings are in agreement with previous investigations

[13, 14]. The size of the crystallites was calculated from the broadening of the anatase (101) peak using the Scherrer equation and was in the range of 33 to 37 nm.

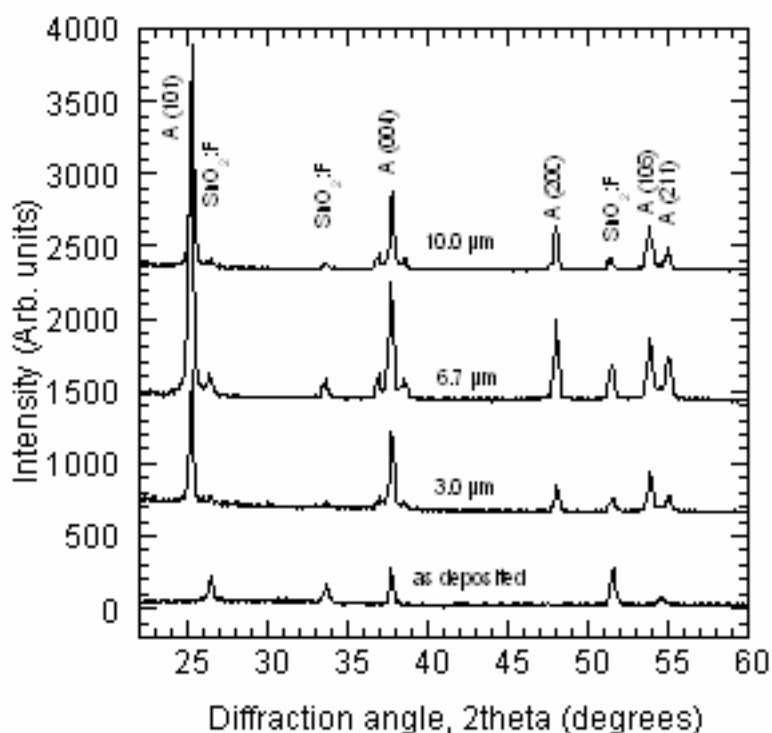
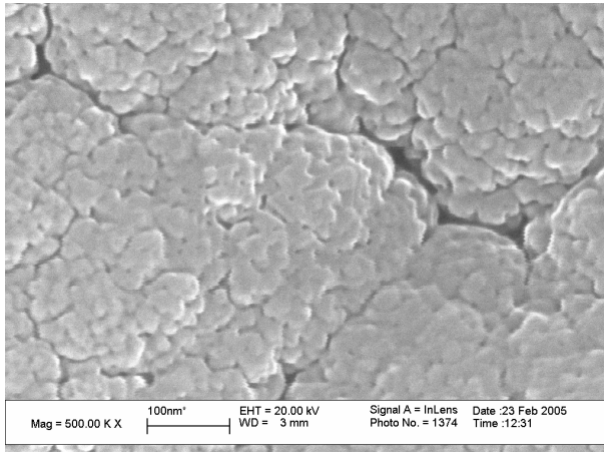


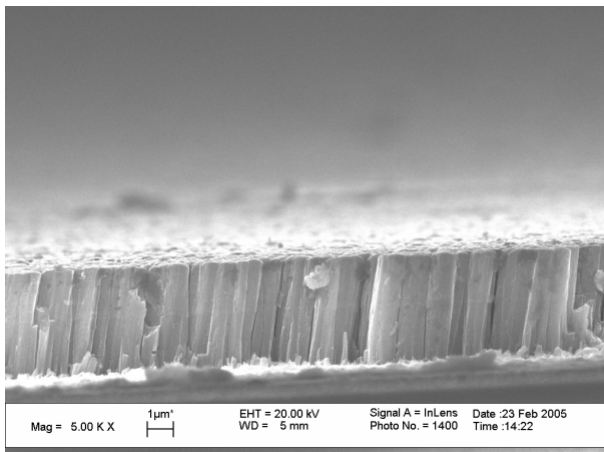
Figure 1. XRD patterns of the sputtered titanium dioxide thin films.

Scanning electron microscopy (SEM) was used to study the morphology of the films. Figure 2 shows the top-down SEM images of the sputtered titanium dioxide films. A cauliflower-like surface with clearly defined particles is visible. The particle size (27-38 nm) is similar to that determined by XRD. Also voids are visible, which are essential for efficient dye-sensitized solar cells. They make the films porous and increase the surface area, so that sufficient dye-absorption in a monolayer can take place. Furthermore, voids can affect the light scattering properties of the film. The

cross-section clearly shows the columnar structure of the film. The columns are slightly tilted ( $\sim 10^\circ$ ) with respect to the substrate normal.



(a)



(b)

Figure 2. Top-down (a) and cross-sectional (b) SEM images of an obliquely sputtered titanium dioxide films

Figure 3 shows the current-voltage characteristics of the dye-sensitized solar cells recorded at 0.1 sun illumination. The photocurrent increases with the film thickness, indicating that light absorption is clearly a limiting factor in these cells. The

roughness factor of the obliquely sputtered  $\text{TiO}_2$  films appears to be significantly lower than that of films prepared from  $\text{TiO}_2$  colloids. The photovoltaic conversion efficiency also increases with film thickness and reached  $\sim 3.3\%$  for the thickest film. This efficiency is comparable to the 4% obtained with sputtered [15] and evaporated [12] films published previously. It is noted that we did not optimize the electrolyte with respect to efficiency. To compare the properties of the sputtered  $\text{TiO}_2$  film with colloid-based  $\text{TiO}_2$  films electron transport and lifetime studies were performed.

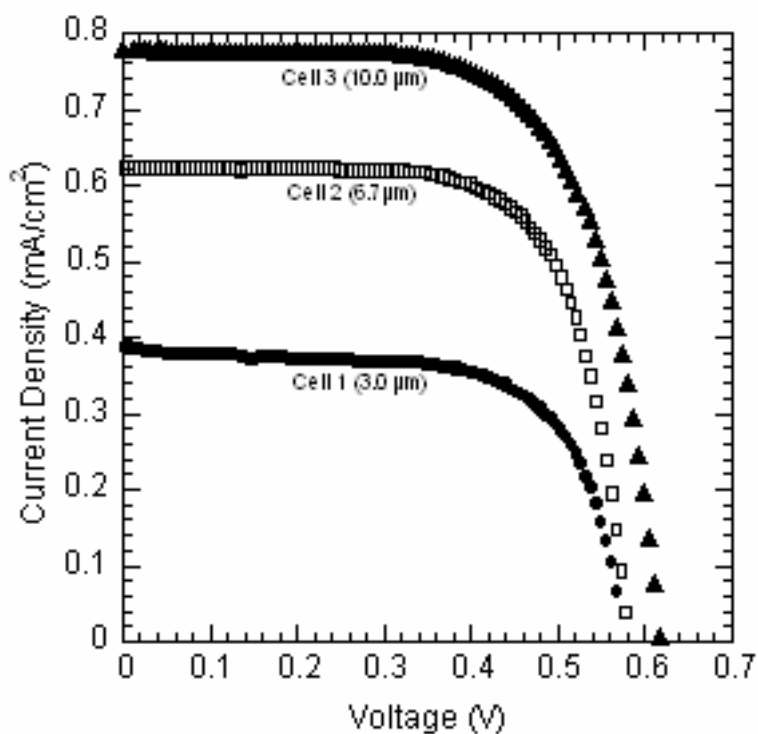
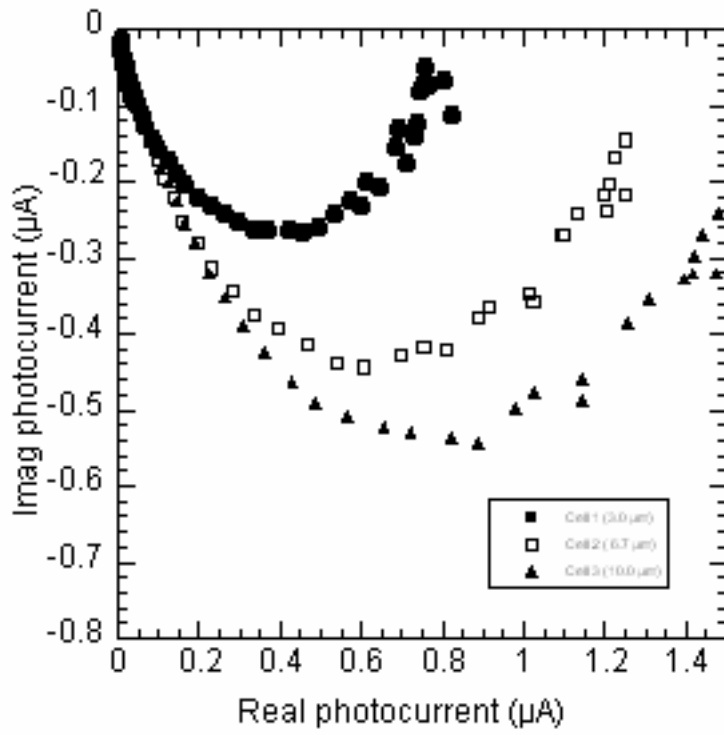


Figure 3. Current-voltage characteristics of dye-sensitized solar cells based on sputtered  $\text{TiO}_2$  films in simulated sunlight (intensity  $100 \text{ W m}^{-2}$ ). The film thickness is indicated.

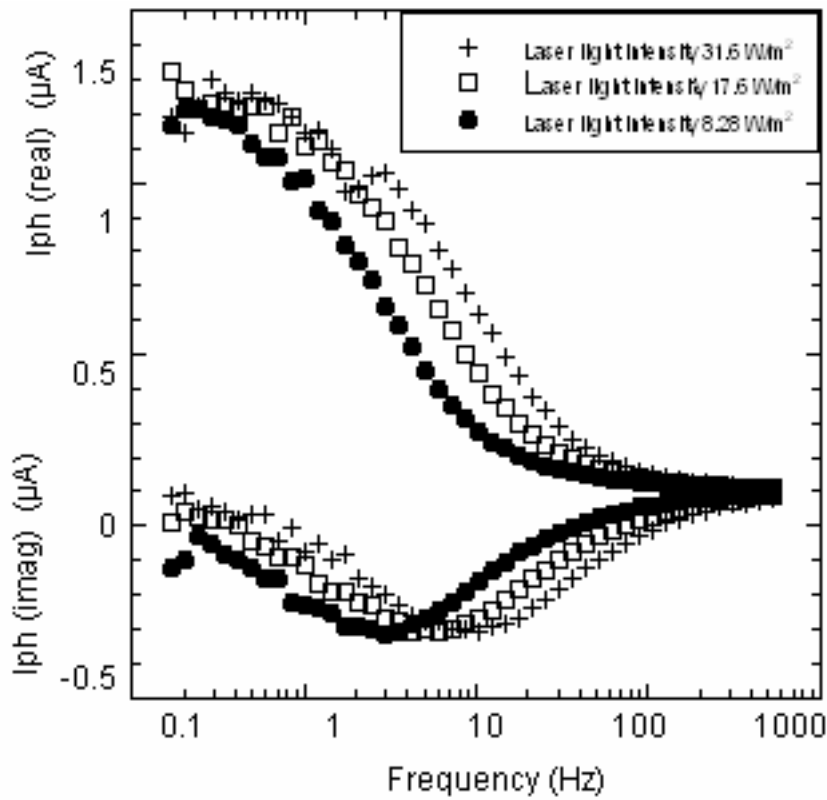
Transport of photoinjected electrons in the sputtered  $\text{TiO}_2$  films was studied using IMPS at short-circuit conditions. Figure 4a shows typical IMPS response for cells with different  $\text{TiO}_2$  film thickness in a complex plane plot. The data forms depressed semicircles that increase in radius with increasing  $\text{TiO}_2$  film thickness. This is a direct result of the larger photocurrents obtained in thicker films. Figure 4b shows the real and imaginary parts of the modulated photocurrent as function of frequency, for one solar cell at different light intensities. It can be seen that the IMPS response shifts toward higher frequencies with increasing light intensities, while the amplitude of the signals remains the same. The general shape and behavior of the IMPS signals is very similar to that recorded for cells prepared from  $\text{TiO}_2$  colloids. A single time constant can be extracted from the IMPS data. Figure 4c shows the IMPS time constants ( $\tau_{\text{IMPS}}$ ) of the 3 cells as function of light intensity. As will be shown later,  $\tau_{\text{IMPS}}$  can be interpreted as the electron transport time. Electron transport becomes more rapid at higher light intensities, as is the case for dye-sensitized solar cells based on colloidal  $\text{TiO}_2$ . This behavior can be explained using a multiple trapping model, in which an exponentially increasing density of traps towards the conduction band is assumed [6, 16]. The transport time increases with film thickness. If diffusion is the driving force for electron transport, one would expect  $\tau_{\text{IMPS}}$  to scale with the square of the film thickness. It appears, however, that  $\tau_{\text{IMPS}}$  for the sputtered  $\text{TiO}_2$  solar cells is proportional to the film thickness.

The number of electrons accumulated in the  $\text{TiO}_2$  under short circuit conditions ( $Q_{\text{SC}}$ ) was determined by charge extraction. Figure 4d displays  $Q_{\text{SC}}$  as function of light intensity.  $Q_{\text{SC}}$  increases with light intensity and with  $\text{TiO}_2$  film thickness. The extracted charge is approximately proportional to the film thickness.  $Q_{\text{SC}}$  for the

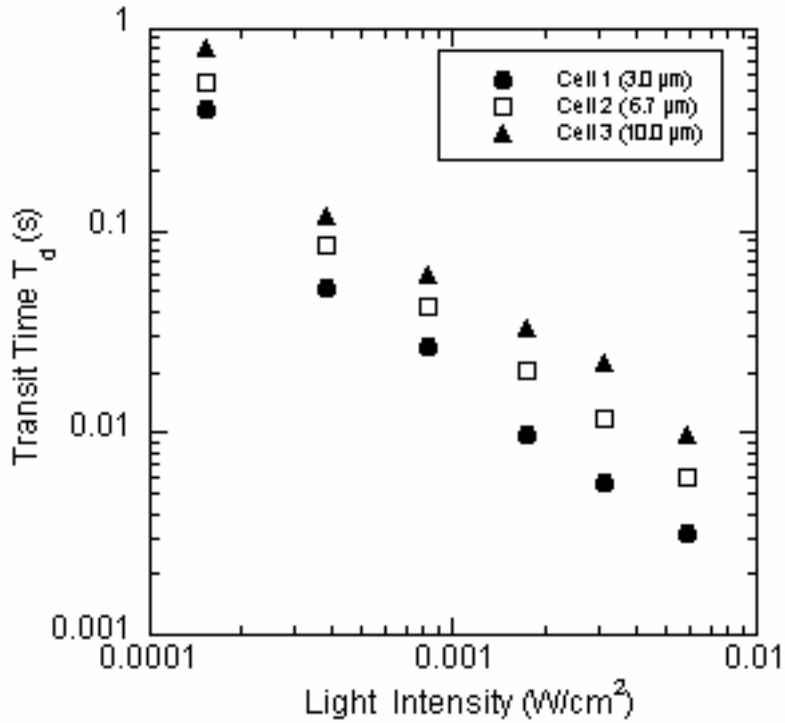
sputtered films is comparable with that determined for films based on colloidal  $\text{TiO}_2$  [17, 18].



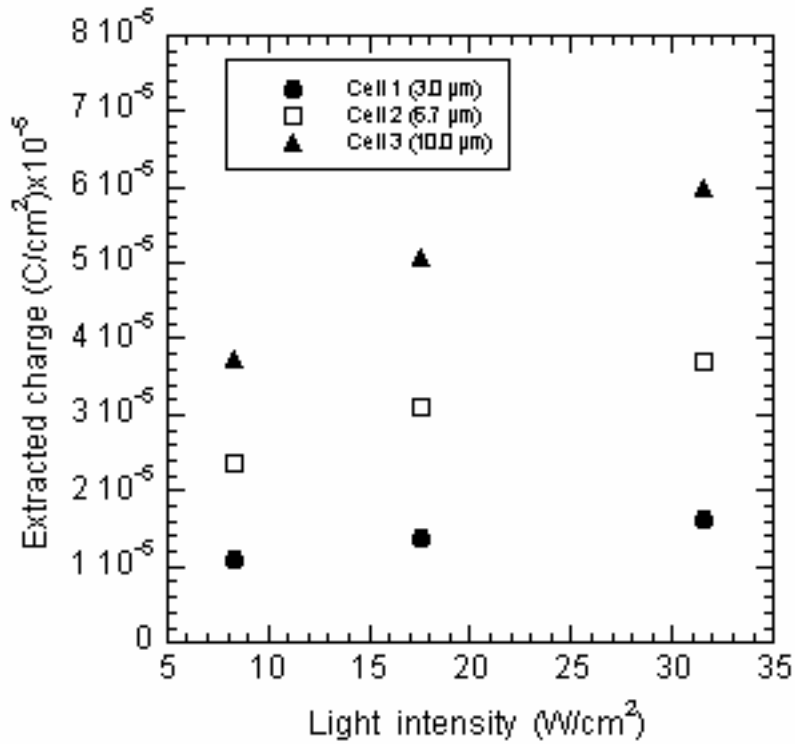
(a)



(b)



(c)



(d)

Figure 4. (a) Complex plane plot of the measured IMPS spectra for the different solar cells at an irradiation equivalent to  $8.28 \text{ W/m}^2$ .

(b) Imaginary and real photocurrents as functions of frequency for cell 2 ( $6.7 \mu\text{m}$ ) irradiated with different laser light intensities.

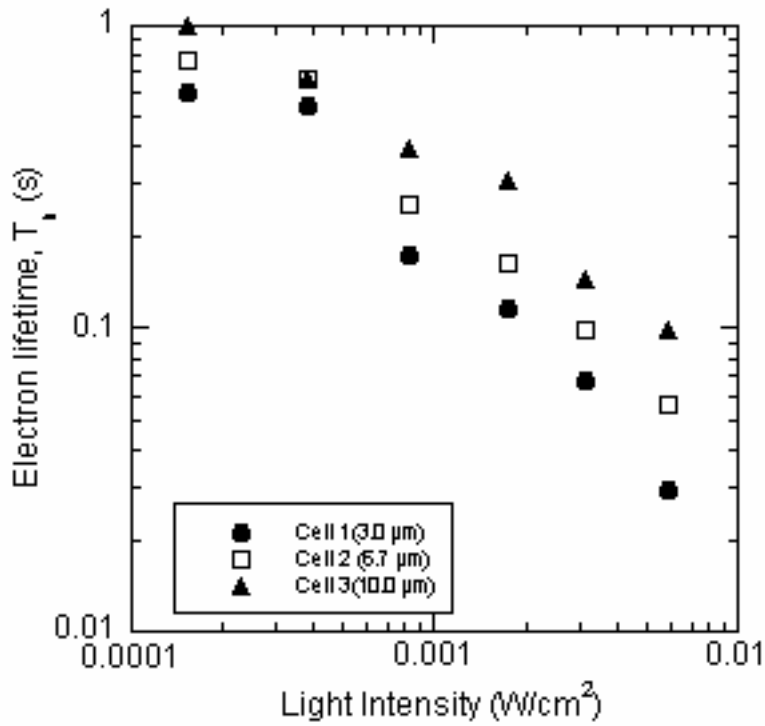
(c) Electron transit time as a function of laser light intensity for all the solar cells.

(d) Accumulated charge in the solar cells under short-circuits conditions as a function of laser light intensity.

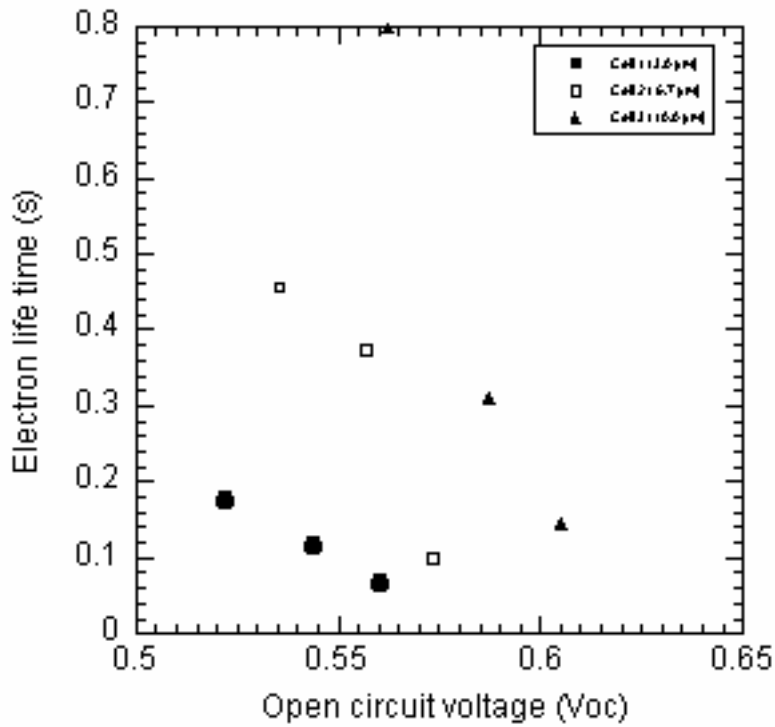
The lifetime of electrons in the sputtered  $\text{TiO}_2$  films was investigated at open circuit conditions using IMVS. IMVS spectra form semicircles in the complex plane (not shown), similar to results from dye-sensitized solar cells based on colloidal  $\text{TiO}_2$  [7].

The time constant extracted from the IMVS data corresponds to the electron lifetime  $\tau_e$  and is shown as function of light intensity in Figure 5a. The electron lifetime is

determined by recombination of electrons in the  $\text{TiO}_2$  with the oxidized part of the redox couple,  $\text{I}_3^-$ .  $\tau_e$  was found to increase with film thickness. Plotting the lifetime against the open circuit potential, Figure 5b, it can be seen that at a given voltage thicker films yield longer lifetimes. As the voltage determines the electron concentration in the  $\text{TiO}_2$  the change in  $\tau_e$  is unexpected. A possible explanation is that the FTO substrate contributes to the back transfer of electrons to the redox couple [19]. This effect will become less important if thicker  $\text{TiO}_2$  films are present.



(a)



(b)

Figure 5. (a) Electron lifetime as a function of laser light intensity for all the solar cells.

(b) Electron lifetime as a function of open circuit voltage for the fabricated solar cells.

It is noted that IMVS times are about one order of magnitude higher than IMPS times at the same light intensities. As the internal potential in the sputtered  $\text{TiO}_2$  will be lower under short circuit conditions than at open circuit, it is clear that the electron lifetime under short circuit condition will be much longer. Recombination of electrons with the triiodide is therefore negligible under short circuit conditions. The relatively

low short circuit photocurrents for the sputtered TiO<sub>2</sub> films are therefore not caused by electron recombination during electron transport.

In conclusion, the properties of dye-sensitized solar cells based on porous TiO<sub>2</sub> films deposited by oblique DC magnetron sputtering have been studied in detail. Electron transport and recombination were found to be very similar to that observed for solar cells based on TiO<sub>2</sub> films prepared by other methods, such as doctor blading or screen printing. Although the different methods yield films with different morphologies, it is noted that they all are composed of a porous assembly of TiO<sub>2</sub> nanocrystals. Grain boundaries with associated trap and / or energy barriers are the likely cause of the observed transport properties.

### **Acknowledgements**

This work was supported by the International Science Program at Uppsala University.

## References

- [1] B. O'Regan, M. Grätzel, *Nature (London)* 353 (1991) 737.
- [2] M. Grätzel, *J. Photochem. Photobiol. C: Photochem.Rev.* 4 (2003) 145–153.
- [3] F. Cao, G. Oskam, P. C. Searson, *J. Phys. Chem.* 100 (1996) 17021.
- [4] P. E. de Jongh, D. Vanmaekelbergh, *Phys. Rev. Lett* 77 (1996) 3427.
- [5] L. Dloczik, O. Ileperuma, I. Lauer mann, L. Peter, E. Ponomarev, G. Redmond, N. Shaw, I. Uhlendorf, *J. Phys. Chem. B* 101 (1997) 10281.
- [6] A. C. Fisher, L. M. Peter, E. A. Ponomarev, A. B. Walker, K. G. U. Wijayantha, *J. Phys. Chem. B* 104 (2000) 949.
- [7] G. Schlichthörl, S. Y. Huang, J. Sprague, A. J. Frank, *J. Phys. Chem. B* 101 (1997) 8139.
- [8] K. D. Benkstein, N. Kopidakis, J. van de Lagemaat, A. J. Frank, *J. Phys. Chem. B* 107 (2003) 7759.
- [9] S. Nakade, Y. Saito, W. Kubo, T. Kitamura, Y. Wada, S. Yanagida, *J. Phys. Chem. B* 107 (2003) 8607.
- [10] J. Rodríguez, M. Gómez, J. Lu, Eva Olsson, C.-G. Granqvist, *Adv. Mater.* 12 (2000) 341.
- [11] M. Gómez, J. Lu, J. L. Solis, E. Olsson, A. Hagfeldt, C. G. Granqvist, *J. Phys. Chem. B* 104 (2000) 8712.
- [12] G. K. Kiema, M. J. Colgan, M. J. Brett, *Sol. Energy Mater. Sol. Cells* 85 (2005) 321–331.
- [13] S. B. Amor, L. Guedri, G. Baud, M. Jacquet, M. Ghedira, *Mater. Chem. Phys.* 77 (2002) 903.
- [14] B. Karunakaran, R. T. R. Kumar, D. Mangalaraj, S. K. Narayandass, G. M. Rao, *Cryst. Res. Technol.* 37 (2002) 1285.
- [15] M. Gómez, J. Lu, E. Olsson, A. Hagfeldt, C. G. Granqvist, *Sol. Energy Mater. Sol. Cells* 64 (2000) 385.
- [16] J. van de Lagemaat, A. J. Frank, *J. Phys. Chem. B* 104 (2000) 4292.
- [17] G. Boschloo, A. Hagfeldt, *J. Phys. Chem. B.* 109 (2005) 12093.
- [18] H. Paulsson, L. Kloo, A. Hagfeldt, G. Boschloo, *J. Electroanal. Chem.* 586 (2006) 56.
- [19] P. J. Cameron, L. M. Peter, *J. Phys. Chem. B* 109 (2005) 7392.

## Figure captions

Figure 1. XRD patterns of the sputtered titanium dioxide thin films.

Figure 2. Top-down and cross-sectional SEM images of an obliquely sputtered titanium dioxide films

Figure 3. Current-voltage characteristics of dye-sensitized solar cells based on sputtered TiO<sub>2</sub> films in simulated sunlight (intensity 100 W m<sup>-2</sup>). The film thickness is indicated.

Figure 4. (a) Complex plane plot of the measured IMPS spectra for the different solar cells at an irradiation equivalent to 8.28 W/m<sup>2</sup>.

(b) Imaginary and real photocurrents as functions of frequency for cell 2 (6.7 μm) irradiated with different laser light intensities.

(c) Electron transit time as a function of laser light intensity for all the solar cells.

(d) Accumulated charge in the solar cells under short-circuits conditions as a function of laser light intensity.

Figure 5. (a) Electron lifetime as a function of laser light intensity for all the solar cells.

(b) Electron lifetime as a function of open circuit voltage for the fabricated solar cells.